Stronger Functional Connectivity in the Default Mode and Salience Networks is Associated with Youthful Memory in Superaging

Jiahe Zhang[1], Joseph Andreano[2,3], Bradford C. Dickerson[3,4,5*†] Alexandra Touroutoglou[3,4,5*] & Lisa Feldman Barrett[1,2,3*†]

[1]Department of Psychology, 125 Nightingale Hall, Northeastern University, Boston, MA 02115
[2]Psychiatric Neuroimaging Division, Department of Psychiatry, Massachusetts General Hospital and Harvard Medical School, 149 13th St., Charlestown, MA 02129
[3]Athinoula A. Martinos Center for Biomedical Imaging, Massachusetts General Hospital and Harvard Medical School, 149 13th St., Charlestown, MA 02129
[4]Department of Neurology, Massachusetts General Hospital and Harvard Medical School, 149 13th St., Charlestown, MA 02129
[5]Frontotemporal Disorders Unit, Department of Neurology, Massachusetts General Hospital and Harvard Medical School, 149 13th St., Charlestown, MA 02129

[*]Made equivalent contributions and share senior authorship.

Supplementary Material

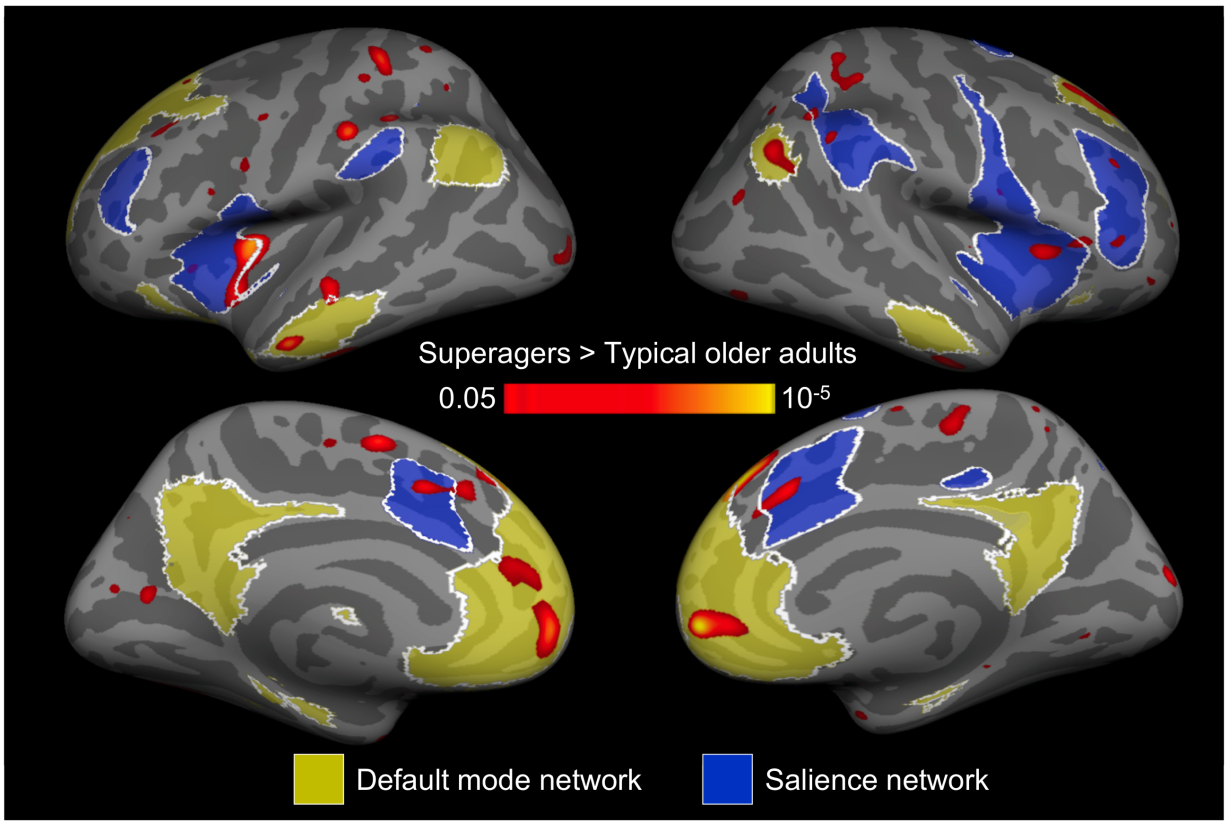

Figure S1. Regions of the DMN (yellow) and SN (blue) where superagers have thicker cortex than typical older adults. Map was thresholded at $p < 0.05$. Figure was adapted from (Sun et al., 2016).

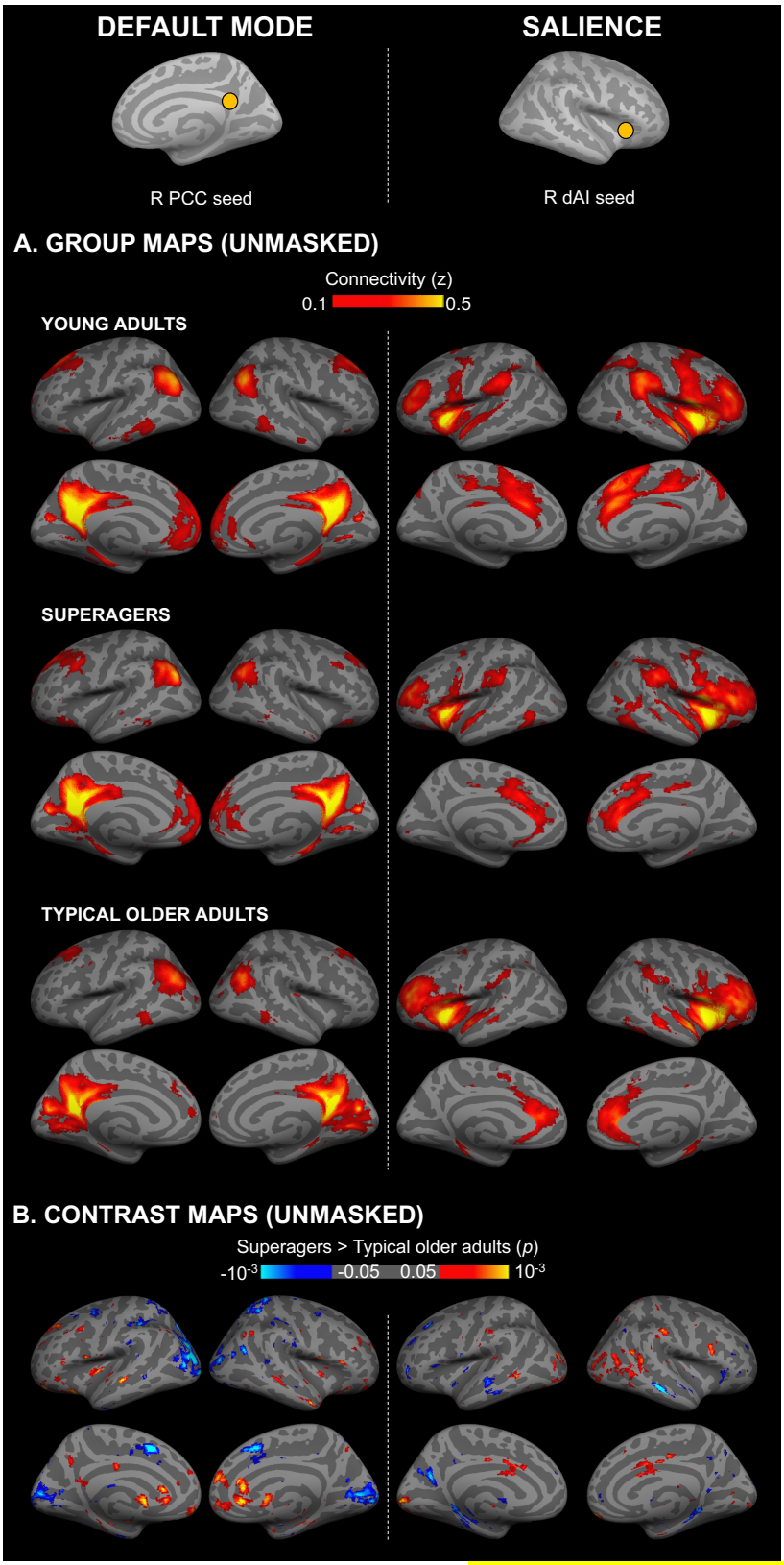

Figure S2. Group and contrast maps. A) Group-averaged DMN and SN map of young adults, superagers and typical older adults ($z > 0.1$). Network seed regions are indicated by orange circles. B) Unmasked contrast maps of superagers versus typical older adults.

Table S1. MNI coordinates of seed and target regions within the default mode, salience and control networks.

Region	MNI coordinates		
	x	y	z
Default mode network			
PCC seed	1	-55	17
L AG	-42	-74	50
L SFG	-16	37	40
L dmPFC	-1	55	15
L rmPFC	-4	56	-13
R AG	54	-57	42
R aMTG	61	5	-29
R vlPFC	35	34	-16
R dmPFC	9	54	19
R pgACC	5	31	12
R sgACC	5	34	-1
R rmPFC	9	46	-6
R HF	27	-22	-18
Salience network			
dAI seed	36	21	1
L MCC	-1	14	28
R MCC	3	6	34
R SMG	56	-25	37
Control networks			
L M1 seed	-43	-16	42
R M1	23	-15	64
L V1 seed	-19	-98	-3
R V1	22	-94	-8

Text S1. Principal component analysis (PCA) and brain-behavior regression model using PCA factor scores.

In the main manuscript, we used a key node approach to summarize network connectivity, i.e. we used connectivity between representative nodes to index functional connectivity of a network or between networks. As a complementary analysis to the key node approach, we also conducted a principal component analysis to examine whether the 17 seed-target connectivity pairs within and between DMN and SN should be decomposed into components drastically different from the known DMN and SN distinction. This includes 12 pairs within DMN, 3 pairs within SN and 2 pairs between DMN and SN. Using the factor analysis function in IBM SPSS Statistics 25 with varimax rotation, we tested and found 2 stable components (Figure S1A) across 17 seed-target connectivity pairs within DMN, within SN and between DMN and SN (Figure S1B). In general, Component 1 appeared to index SN and Component 2 appeared to index DMN, because connectivity pairs canonical SN seed-target pairs (i.e. R MCC-R dAI, L MCC-R dAI and R SMG-R dAI) loaded high on Component 1 and low on Component 2 while canonical DMN seed-target pairs (i.e. L dmPFC-R PCC, R dmPFC-R PCC and R HF-R PCC) loaded low on Component 1 and high on Component 2. Interestingly, between-network connectivity pairs (i.e. L MCC-R PCC and R MCC-R PCC) loaded extremely low on both components.

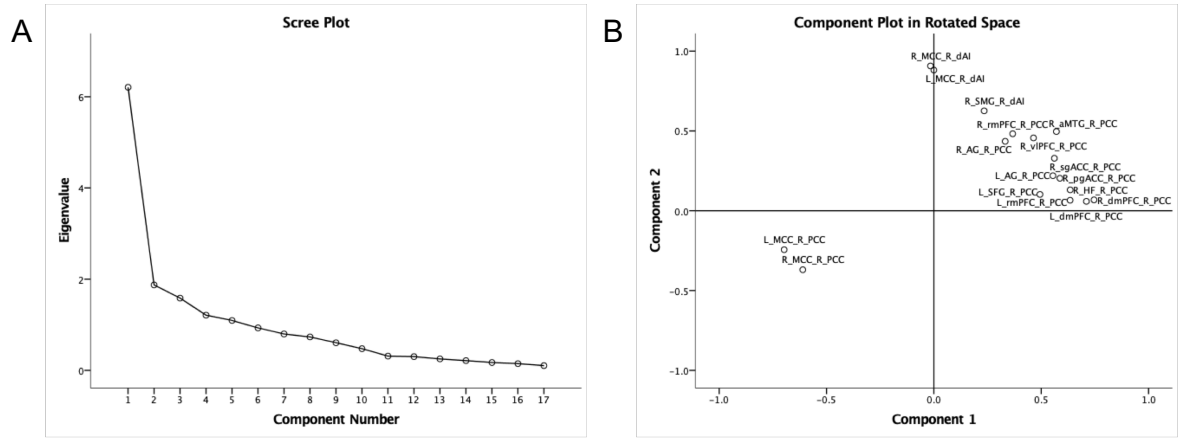

Figure S3. PCA results. Using PCA, we tested and found 2 stable components across 17 seed-target connectivity pairs within DMN, within SN and between DMN and SN. A) The scree plot plots eigenvalue as a function of increasing number of components. This plot had an 'elbow' at 2, since further addition of components did not add substantial explained variance. B) Component 1 appeared to index SN connectivity while Component 2 appeared to index DMN connectivity.

Text S2. Brain-behavior regression models using cortical thickness extracted from functional connectivity ROIs.

To verify that the regression analyses including cortical thickness estimates as predictors were not confounded 1) by ROI location and 2) by excluding ROIs that did not differ in thickness between superagers and typical older adults (Sun et al., 2016), we conducted regression analyses including cortical thickness estimates extracted 1) from the same ROIs as the functional connectivity seed and targets, and 2) from seeds and targets that did not differ in cortical thickness between superagers and typical older adults. Instead of using the ROIs created for functional connectivity calculations (which did not provide the best cortical thickness estimates due to their set 4mm spherical shape), we matched the ROIs to their corresponding parcels in a standard parcellation scheme (Glasser et al., 2016) (R PCC: R_v23ab; R dAI: R_AVI_ROI; L MCC: L_a24pr). We extracted the cortical thickness values of these parcels and regressed out the mean cortical thickness to obtain the residual cortical thickness values, similar to (Sun et al., 2016). These parcels did not differ in residual cortical thickness between superagers and typical older adults (R PCC: $t = -0.03$, $p = 0.97$; R dAI: $t = 0.05$, $p = 0.96$; L MCC: $t = -0.45$, $p = 0.66$, two-tailed t-test).

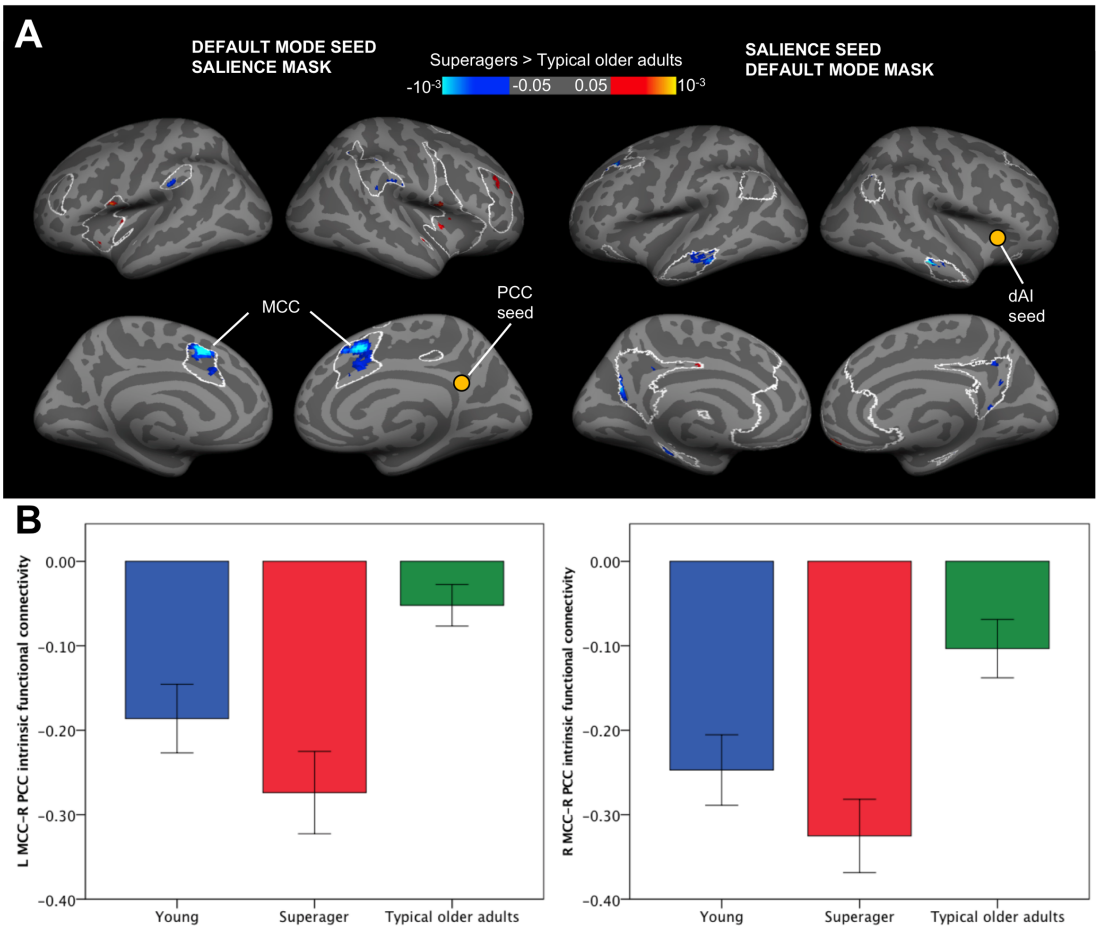

Figure S4. Between-network connectivity differences. A) Regions of the DMN and SN (outlined in white) where superagers had higher between-network connectivity (red/yellow) or lower between-network connectivity (blue-cyan) than did typical older adults. Notably, bilateral MCC, a key superaging region consistently showing greater cortical thickness across multiple studies (Harrison et al., 2012; Rogalski et al., 2013; Gefen et al., 2014; Sun et al., 2016), was more strongly inversely correlated with the PCC seed in superagers compared to typical older adults. Other regions showing group differences include bilateral SMG, right MFG, and bilateral mid insula from the SN, as well as bilateral MTG and PCC from the DMN. For each network, a two-sample t-test between superagers and typical older adults was conducted. Maps were thresholded at $p < 0.05$ and masked by the opposite network. B) Bar graphs show that in superagers and young adults, the MCC was more strongly inversely correlated with PCC compared to typical older adults ($p < 0.05$). There was no difference in MCC-PCC connectivity strength between superagers and young adults. We calculated intrinsic connectivity strength between the right PCC seed and bilateral MCC targets identified from peaks in the t-test maps in panel A. R, right hemisphere; L, left hemisphere. Error bars indicate 1 standard error of the mean.

Table S2. Association between memory and intrinsic connectivity *between* DMN and SN.

Target-Seed	Recall		Item Recognition		Associative Recognition	
	r	*p*	*r*	*p*	*r*	*p*
L MCC-R PCC	-0.39	0.01**	-0.45	0.00**	-0.36	0.01*
R MCC-R PCC	-0.47	0.00**	-0.17	0.15	-0.08	0.32

Note: *r* = Pearson's correlation coefficients, *p* = one-tailed significance. Uncorrected significance: * $p < 0.05$, ** $p < 0.01$.

Table S3. Association between memory and intrinsic connectivity within control networks.

Control networks	Recall		Item recognition		Associative recognition	
	r	*p*	*r*	*p*	*r*	*p*
Motor network	0.43	0.01**	0.25	0.12	0.18	0.26
Visual network	0.21	0.20	0.17	0.28	0.12	0.48

Note: *r* = Pearson's correlation coefficients, *p* = two-tailed significance. Uncorrected significance: * $p < 0.05$, ** $p < 0.01$.

Table S4. Stronger functional connectivity in the DMN and in the SN independently predicted better recall memory and item recognition memory performance in older adults.

	Recall memory performance			
	B	*t*	R^2 change	Total R^2
R HF-R PCC connectivity[a]	0.31	2.19	0.10	0.28
L MCC-R dAI connectivity[b]	0.41	2.85	0.17	
	Item recognition memory performance			
	B	*t*	R^2 change	Total R^2
R HF-R PCC connectivity[c]	0.26	1.71	0.07	0.15
L MCC-R dAI connectivity[d]	0.28	1.79	0.08	

Note: This table displays standardized regression coefficient (*B*), t statistic (*t*), incremental variance (R^2 change), as well as total variance (Total R^2) in recall memory performance predicted by entering both independent variables into a single multiple linear regression model. Incremental R^2 change indicates additional variance explained by respective independent variable when entered last in the model. [a]$p = 0.04$, [b]$p = 0.01$, [c]$p = 0.10$, [d]$p = 0.08$.

Table S5. Stronger functional connectivity between the DMN and in the SN independently predicted better item recognition memory performance in older adults.

	Item recognition memory performance			
	B	*t*	R^2 change	Total R^2
R HF-R PCC connectivity[a]	0.10	0.62	0.01	0.26
L MCC-R dAI connectivity[b]	0.23	1.56	0.05	
L MCC-R PCC connectivity[c]	-0.37	-2.26	0.11	

Note: This table displays standardized regression coefficient (*B*), t statistic (*t*), incremental variance (R^2 change), as well as total variance (Total R^2) in item recognition memory performance predicted by entering both independent variables into a single multiple linear regression model. Incremental R^2 change indicates additional variance explained by respective independent variable when entered last in the model. [a]$p = 0.54$, [b]$p = 0.13$, [c]$p = 0.03$.

Table S6. Within DMN and SN, higher structural integrity and stronger intrinsic connectivity independently predicted better recall memory in the older adults.

	Recall memory performance			
	B	*t*	R^2 change	Total R^2
Default mode network				
Adjusted R hippocampal volume[a]	0.40	2.73	0.16	0.27
R HF-R PCC connectivity[b]	0.30	2.08	0.09	
Salience network				
Adjusted L MCC thickness[c]	0.29	1.92	0.08	0.26
L MCC-R dAI connectivity[d]	0.35	2.34	0.12	

Note: This table displays standardized regression coefficient (*B*), t statistic (*t*), incremental variance (R^2 change), as well as total variance (Total R^2) in recall memory performance predicted by entering both independent variables into a single multiple linear regression model. Incremental R^2 change indicates additional variance explained by respective independent variable when entered last in the model. [a]$p = 0.01$, [b]$p = 0.05$, [c]$p = 0.06$, [d]$p = 0.03$.

Table S7. Combining both DMN and SN, higher structural integrity and stronger functional connectivity independently predicted better recall memory performance in older adults.

	Recall memory performance			
	B	*t*	R^2 change	Total R^2
Structural estimates[a]			0.15	0.44
Adjusted R hippocampal volume[c]	0.35	2.60		
Adjusted L MCC thickness[d]	0.21	1.48		
Functional estimates[b]			0.13	
R HF-R PCC connectivity[e]	0.22	1.63		
L MCC-R dAI connectivity[f]	0.31	2.26		

Note: This table displays standardized regression coefficient (*B*), t statistic (*t*), incremental variance (R^2 change), as well as total variance (Total R^2) in recall memory performance predicted by entering both independent variables into a single multiple linear regression model. Incremental R^2 change indicates additional variance explained by respective block of independent variables when entered last in the model. *p* values for each block of variables: [a]p = 0.02, [b]p = 0.03. *p* values for each independent variable: [c]p = 0.01, [d]p = 0.15, [e]p = 0.11, [f]p = 0.03.

Table S8. Combined DMN and SN regression model incorporating functional connectivity estimates derived from PCA.

	Recall memory performance			
	B	*t*	R^2 change	Total R^2
Structural estimates[a]			0.07	0.49
Adjusted R hippocampal volume[c]	0.26	1.96		
Adjusted L MCC thickness[d]	0.13	0.93		
Functional estimates[b]			**0.18**	
PCA factor score 1 ('SN')[e]	**0.36**	**2.60**		
PCA factor score 2 ('DMN')[f]	**0.35**	**2.57**		

Note: This table displays standardized regression coefficient (*B*), t statistic (*t*), incremental variance (R^2 change), as well as total variance (Total R^2) in recall memory performance predicted by entering both independent variables into a single multiple linear regression model. Incremental R^2 change indicates additional variance explained by respective block of independent variables when entered last in the model. *p* values for each block of variables: [a]p = 0.13, **[b]p = 0.01**. *p* values for each independent variable: [c]p = 0.06, [d]p = 0.36, **[e]p = 0.01, [f]p = 0.02**.

Table S9. Within-network regression models incorporating volume and thickness estimates of functional connectivity ROIs.

	Recall memory performance			
	B	*t*	R^2 change	Total R^2
Default mode network				
Adjusted R hippocampal volume[a]	0.43	2.80	0.16	0.28
Adjusted R PCC thickness[b]	-0.11	-0.73	0.01	
R HF-R PCC connectivity[c]	**0.29**	**1.96**	**0.08**	
Salience network				
Adjusted L MCC thickness[d]	0.03	0.17	0.00	0.19
Adjusted R dAI thickness[e]	0.07	0.40	0.00	
L MCC-R dAI connectivity[f]	**0.42**	**2.52**	**0.15**	

Note: This table displays standardized regression coefficient (*B*), t statistic (*t*), incremental variance (R^2 change), as well as total variance (Total R^2) in recall memory performance predicted by entering both independent variables into a single multiple linear regression model. Incremental R^2 change indicates additional variance explained by respective independent variable when entered last in the model. [a]$p = 0.01$, [b]$p = 0.47$, [c]$\mathbf{p = 0.06}$, [d]$p = 0.08$, [e]$p = 0.69$, [f]$\mathbf{p = 0.02}$.

Table S10. Combined DMN and SN regression model incorporating volume and thickness estimates of functional connectivity ROIs.

	Recall memory performance			
	B	*t*	R^2 change	Total R^2
Structural estimates[a]			0.13	0.42
Adjusted R hippocampal volume[c]	0.36	2.38		
Adjusted R PCC thickness[d]	-0.02	-0.16		
Adjusted L MCC thickness[e]	-0.03	-0.21		
Adjusted R dAI thickness[f]	0.13	0.91		
Functional estimates[b]			**0.18**	
R HF-R PCC connectivity[g]	**0.31**	**2.16**		
L MCC-R dAI connectivity[h]	**0.31**	**1.99**		

Note: This table displays standardized regression coefficient (*B*), t statistic (*t*), incremental variance (R^2 change), as well as total variance (Total R^2) in recall memory performance predicted by entering both independent variables into a single multiple linear regression model. Incremental R^2 change indicates additional variance explained by respective block of independent variables when entered last in the model. *p* values for each block of variables: [a]p = 0.16, **[b]p = 0.02**. *p* values for each independent variable: [c]p = 0.02, [d]p = 0.87, [e]p = 0.84, [f]p = 0.37**, [g]p = 0.04, [h]p = 0.06.**

References

Gefen T, Shaw E, Whitney K, Martersteck A, Stratton J, Rademaker A, Weintraub S, Mesulam MM, Rogalski E (2014) Longitudinal Neuropsychological Performance of Cognitive SuperAgers. Journal of the American Geriatrics Society 62:1598-1600.

Glasser MF, Coalson TS, Robinson EC, Hacker CD, Harwell J, Yacoub E, Ugurbil K, Andersson J, Beckmann CF, Jenkinson M, Smith SM, Van Essen DC (2016) A multi-modal parcellation of human cerebral cortex. Nature 536:171-178.

Harrison TM, Weintraub S, Mesulam MM, Rogalski E (2012) Superior Memory and Higher Cortical Volumes in Unusually Successful Cognitive Aging. Journal of the International Neuropsychological Society 18:1081-1085.

Rogalski EJ, Gefen T, Shi J, Samimi M, Bigio E, Weintraub S, Geula C, Mesulam MM (2013) Youthful Memory Capacity in Old Brains: Anatomic and Genetic Clues from the Northwestern SuperAging Project. Journal of Cognitive Neuroscience 25:29-36.

Sun FW, Stepanovic MR, Andreano J, Barrett LF, Touroutoglou A, Dickerson BC (2016) Youthful Brains in Older Adults: Preserved Neuroanatomy in the Default Mode and Salience Networks Contributes to Youthful Memory in Superaging. The Journal of neuroscience : the official journal of the Society for Neuroscience 36:9659-9668.